NEW VLA OBSERVATIONS OF THE HH 1-2 REGION: EVIDENCE FOR DENSITY ENHANCEMENTS MOVING ALONG THE AXIS OF THE VLA 1 RADIO JET

Luis F. Rodríguez[1], Víctor G. Delgado[1,2], Yolanda Gómez[1], Bo Reipurth[3], José M. Torrelles[4], Alberto Noriega-Crespo[5], Alejandro C. Raga[1], and Jorge Cantó[1]

[1]Instituto de Astronomía, UNAM, Apdo. Postal 70-264, México, DF, 04510, México

[2]Instituto de Física y Matemáticas, UMSNH, Ciudad Universitaria, Edificio "C3", Morelia, Mich., 58040, México

[3]Center for Astrophysics and Space Astronomy, Campus Box 389, University of Colorado, Boulder, CO 80309, USA

[4]Institut d'Estudis Espacials de Catalunya (IEEC/CSIC), Edifici Nexus, C/ Gran Capita 2-4, E-08034 Barcelona, Spain

[5]Infrared Processing and Analysis Center, California Institute of Technology-JPL, Pasadena, CA 91125, USA

Received _____; accepted _____

Submitted to The Astronomical Journal, August, 1999

ABSTRACT

Using the Very Large Array, we have carried out new, sensitive radio continuum observations at 6 and 3.6 cm of the HH 1-2 region. The comparison between the 6-cm maps made from data taken in 1986.2 and 1992.9 indicates that VLA 1, the exciting source of the HH 1-2 flow, has suffered a morphological change that is attributed to the motion of a symmetric pair of knots along the axis of the radio jet. The proper motion of these knots, that are observed within one arc sec from the embedded star, are consistent with the values found for optical and near-IR jets several arc seconds away. Furthermore, we are able to show that one of the knots observed in the 1986.2 radio data has emerged out of the heavily obscured region around VLA 1 as a near-infrared knot in the 1998.2 data of Reipurth et al. (2000). This result supports the interpretation that the knots are formed by intrinsic processes in the acceleration and collimation of the flow and not by interactions with the surrounding medium. The source VLA 3, associated with an H_2O maser and powering a molecular outflow, also shows morphological changes that we attribute to the turning-on of a new, faint component. Our sensitive 3.6-cm map reveals the presence of a new source, VLA 4, that coincides positionally with the infrared Source 3 of Reipurth et al. (1993). Finally, we derive a proper motion for HH 1F that agrees closely with the optical values. In the case of HH 2 the complexity of the source hampers a detailed comparison with the optical proper motions.

Subject headings: ISM: jets and outflows— ISM: individual (HH 1-2)— Stars: Pre-Main-Sequence

1. Introduction

The bright Herbig-Haro (HH) objects HH 1 and 2 have, since their discovery by Herbig (1951) and Haro (1952), been the focus of a wide variety of detailed studies, and much of our knowledge about HH flows is due to these two objects. This is in part thanks to their great brightness, but, more importantly, because HH 1 and 2 are prototypical cases of the HH phenomenon, displaying two bright bow shocks which move in a bipolar flow away from a central source, which drives a fine collimated jet. Most recently, observations of HH 1 and 2 with the *Hubble Space Telescope* have provided images of unprecedented resolution (e.g. Hester, Stapelfeldt, Scowen 1998, Reipurth et al. 1999, Bally et al. 2000).

Detailed spectroscopic studies have shown that both HH 1 and 2 are high-excitation objects, with low radial velocities (e.g. Böhm & Solf 1985, Solf et al. 1991). Combined with the high proper motions of several hundred km sec^{-1} of the two objects (Herbig & Jones 1981), it follows that they are moving very close to the plane of the sky.

The driving source of the HH 1-2 complex suffers such a high extinction that it is not detected at optical and near-infrared wavelengths. It was first detected as a cm radio continuum source, VLA 1 (Pravdo et al. 1985). Subsequent higher resolution and higher sensitivity data have shown that the source powers a tiny thermal radio jet flowing along the axis of the HH flow (Rodríguez et al. 1990).

Bohigas et al. (1985) and Strom et al. (1985) discovered a small optical jet emanating from the VLA 1 source. Subsequently, a second HH flow, HH 144, was found at a large angle to the HH 1 flow axis, and originating in a second source, VLA 2, located only 3″ from VLA 1 (Reipurth et al. 1993).

Due to the high extinction which often obscures newly born stars, radio continuum observations have emerged as an important tool for the detection of very young stars, and

a large number of embedded jet sources have by now been detected at cm wavelengths (e.g. Anglada et al. 1992, 1998, Rodríguez & Reipurth 1996, 1998). The Herbig-Haro objects themselves have in a few cases been detected at cm wavelengths, including HH 1-2 (Rodríguez et al. 1990), HH 32 (Anglada et al. 1992), HH 12 (Curiel 1995; Rodríguez et al. 1999), and HH 80-81 (Rodríguez & Reipurth 1989).

In this paper, we present very high sensitivity 6 and 3.6 cm radio continuum maps of the region around HH 1-2 and their energy source, and we report the detection of a new VLA source, as well as the hitherto most detailed radio continuum maps of HH 1 and 2, the central thermal radio jet, and several other sources in the region.

2. Observations

The observations were carried out using the Very Large Array (VLA) of the National Radio Astronomy Observatory (NRAO)[1] . In addition to the 6-cm data taken in 1986 and discussed by Rodríguez et al. (1990), we obtained new observations at 3.6 and 6-cm taken in 1992 and 1993. For all the observations the phase center was at the position $\alpha(1950) = 05^h33^m57^s.0$; $\delta(1950) = -06°47'57''.0$, and an effective bandwidth of 100 MHz with two circular polarizations was employed. In all epochs, 1328+307 was the absolute amplitude calibrator and 0539−057 was the phase calibrator. The data were edited and calibrated using the software package Astronomical Image Processing System (AIPS) of NRAO.

In Table 1 we present a summary of the observations that will be discussed here, including the bootstrapped flux density of 0539−057 for each epoch. In the period between

[1]NRAO is a facility of the National Science Foundation operated under cooperative agreement by Associated Universities, Inc.

1986 and 1992, the nominal position of 0539−057 was refined, implying a change of $\Delta\alpha = +0^{s}.0019$ and $\Delta\delta = +0''.07$ from the first to the second epoch. All data were aligned to the new 0539−057 position. This explains the small, systematic shifts between our positions for "stationary" sources and those reported by Rodríguez et al. (1990).

Since no changes were evident in data taken with a time separation of a few months, to obtain the maximum signal to noise ratio we concatenated the data in three files. At 6-cm we have two final files, all from A configuration data: 1986.2 (1986 Mar 01+ 1986 Mar 03) and 1992.9 (1992 Nov 02+ 1992 Dec 18+ 1992 Dec 19). At 3.6-cm we have one final file: 1993.0 (1992 Nov 02+ 1992 Dec 18+ 1992 Dec 19 + 1993 Apr 30). The last epoch of the 3.6-cm data was taken in configuration B, to add short spacings to these data and allow a more reliable comparison with the lower angular resolution 6-cm data. For maps made with natural weighting all three data sets gave angular resolutions of $\sim 0''.5$ and rms noises of 11 μJy (1986.2), 9 μJy (1992.9), and 6 μJy (1993.0). With these three data sets we can address several issues in this region. First, by comparing the 6-cm 1986.2 and 1992.9 maps, we can measure in the radio the proper motions of the Herbig-Haro objects and search for time variability in flux density and morphology over a period of several years in the sources. Second, using the 6-cm 1992.9 map and the 3.6-cm 1993.0 map, we can determine the spectral indices of the sources. Finally, the more sensitive new maps can reveal the presence of fainter sources in the region.

In the natural weight maps for the three data sets, we detect a total of ten sources in a region of $4' \times 4'$ centered at the position of VLA 1, the exciting source of the HH 1-2 system. These sources are shown in Figure 1 and their parameters are given in Table 2.

3. Comments on Individual Sources

In this section we will discuss the radio continuum sources listed in Table 2. We guide our discussion of the sources using the result that radio sources with spectral indices larger than -0.1 are most likely free-free emitters and appear systematically associated with embedded objects (Anglada et al. 1998). Following these authors, we refer to sources with spectral indices larger than -0.1 as sources with "positive" spectral index. We will maintain the nomenclature generally followed in the literature for the two sources at the center of the map, using the names VLA 1 and VLA 2 for this double source (see Figure 2) that has been proposed to form a binary by Reipurth et al. (1993). Also following the usage of previous papers (Chernin & Masson 1995; Choi & Zhou 1997; Correia, Griffin, & Saraceno 1997; Moro-Martín et al. 1999) we will use the name VLA 3 for the more remote radio continuum source to the SW of HH 1 that is associated with a water maser (Rodríguez et al. 1990; Ho et al. 1982). In addition, our sensitive maps reveal the presence of an unreported faint source close to the center of the field, that we will refer to as VLA 4 (see Figure 2). For the remaining six sources, we will extend this nomenclature calling the sources VLA 5 to VLA 10, in order of increasing right ascension.

3.1. VLA 1

This source is believed to be responsible for the excitation of the HH 1-2 system (Pravdo et al. 1985). The 6-cm total flux densities from 1986.2 and 1992.9 agree very closely (see Table 2). This, however, does not exclude the possibility that small morphological variations may have taken place. In their detailed study of the thermal jet that excites the HH 80-81 system, Martí, Rodríguez, & Reipurth (1998) find that, although the total flux density of the source varies by less than $\sim$10%, the detailed comparison of maps made at different epochs reveals the presence of faint condensations moving in the jet. In an attempt

to search for morphology variations in VLA 1 between these two epochs, we undertook several comparisons of the two 6-cm data sets. To obtain the half-power widths and position angle of VLA 1, we did Gaussian ellipsoid fits to the u,v data using the task UVFIT of AIPS, for all three data sets. The result of these fits is given in Table 3. We note that the 6-cm angular size of the major axis of VLA 1 for 1992.9 seems to be significantly smaller than in 1986.2. The upper limits for the angular size of the minor axis of the thermal jet are consistent with the angular size of 0.″11 extrapolated for the base of the jet from the width of the optical and near-infrared knots as a function of distance (Reipurth et al. 2000).

A more direct comparison of the two 6-cm maps of VLA 1 comes from the subtraction of the images. As discussed in detail by Martí et al. (1998), this is no easy task. The main problem is how to align accurately the maps made with data of different epochs before subtracting them. Even a small phase error implying an alignment error of a few tens of milliarcseconds is able to produce strong, meaningless residuals in the difference maps. Indeed, for a source with a convolved (intrinsic source angular size convolved with instrumental angular resolution) angular size of θ and peak flux density of S, a misalignment of $\Delta\theta$ will produce residuals of order $\Delta S \simeq S(\Delta\theta/\theta)$. Since (as will be seen later) we need to measure signals in the difference maps about 10 times weaker than the peak values of individual maps, we require to align the maps to better than one tenth the beam size (our beam size is $\sim 0.''5$, so we need to align the images to better than $\sim 0.''05$). A comparison of the 1986.2 and 1992.9 maps at 6-cm indicates that the positions of the "stationary" (that is, the sources that are not expected to show significant proper motions) sources like VLA 1, VLA 2, and VLA 6, repeat to within $\sim 0.''06$ or better. However, even a shift this small will produce meaningless residuals. In an attempt to align the images better we have followed the least-squares procedure of Martí et al. (1998). First, we made maps for the two epochs using a restoring clean beam with dimensions $0.''63 \times 0.''52$, PA $= -10°$, the average of the synthesized beams for the two epochs. This procedure helps to minimize spurious residuals

in the difference or subtraction maps due to differences in the beams. Since the differences in the individual beam parameters were quite small in our case, of order a few percent, this procedure appears adequate. After this, the 6-cm 1992.9 image was kept fixed as the reference epoch and the 6-cm 1986.2 image was systematically shifted by different amounts and a grid of difference maps (1992.9-1986.2) was computed. The range of shifts explored varied within ± 2 pixel, or ± 120 mas, in each coordinate direction. The linear geometric transformation task LGEOM in AIPS was used repeatedly for such purpose, with a shift step of 0.1 pixel or 6 milliarcsec. The difference maps were computed using the AIPS task COMB for image combining. The procedure adopted to select the shifts leading to the best subtracted image was minimization of the residuals with an rms criterion. This appears to be a reasonable assumption since one expects that a difference image computed with wrong shifts would produce significant positive and/or negative residuals, thus increasing significantly its rms "noise". The rms "noise" is measured here using the IMSTAT task of AIPS for image statistics inside a rectangular window. The window is centered on the central source with a size sufficient to include the complete jet core, and with its major axis being parallel to the direction of the jet.

The shifts that were found to provide the minimum rms noise in the subtracted images were $\Delta\alpha = -0\farcs04$ and $\Delta\delta = -0\farcs05$. The alignment correction required is therefore of the order of a few tens of milliarcsec. The individual maps as well as the resulting best difference images are shown in Fig. 3. The individual maps show some evidence of wiggling along the jet axis. This could be produced by the presence of a very close companion to VLA 1, as has been proposed for the exciting source of the HH 111 flow (Reipurth et al. 1999).

The difference map shows, as statistically significant features, two negative regions. We tentatively interpret these negative regions to imply the presence of emission in 1986.2 that

is no longer present in 1992.9. This emission could be coming, as in the case of HH 80-81, from density enhancements traveling in the jet. Indeed, the 1992.9 map (see Fig. 3) shows faint protuberances at about 1 arc sec from each side of the center of the core. If these faint protuberances are the density enhancements seen closer to the jet center in 1986.2, their proper motion is of order $0\farcs2$ yr^{-1}. Our interpretation is strengthened because the proper motions derived for the HH objects (see below) are similar. If these density enhancements do not change their flux density as they move along the jet, we would expect to see them as positive features in the difference map. However, as discussed by Martí et al. (1998), the flux density of these density enhancements, as they expand with displacement, is expected to drop as their distance to the center of the jet squared. Thus, they become very difficult to detect in the radio once away from the center of the jet. The presence of discrete knots in the near-infrared and optical jet with regular separations that correspond to about four years is well known (Hester et al. 1998; Reipurth et al. 2000). Assuming that the condensation to the NW of the jet moves with a proper motion of $0\farcs18$ year^{-1}, as is the case of HH 1F (see below), we estimate that by 1998.2, the epoch of the near-IR observations of Reipurth et al. (2000), the knot should appear at about $2\farcs7$ from the center of the radio jet. *Remarkably, this is the position of the [FeII] knot L, the closest to the radio source.* We then tentatively identify the NW radio knot deduced from the observations presented in Fig. 3 with knot L in the near-infrared images of Reipurth et al. (2000).

Of course, given the location of the dense molecular gas around VLA 1 (Torrelles et al. 1994), we do not expect to detect in the optical or even infrared wavelengths the heavily obscured SE ejecta.

The existence of density enhancements that travel from very close to the star, at least from $0\farcs5$ from the star (Fig. 3) to several arcsec away (Reipurth et al. 2000) maintaining their identity supports the interpretation that these knots are formed by intrinsic processes

in the acceleration and collimation of the flow, possibly as a result of instabilities in the accretion disk, and not by interactions with the surrounding medium.

From the 1992-3 data at 6 and 3.6-cm, we derive a frequency dependence for the major axis of $\theta_{maj} \propto \nu^{-0.2\pm0.2}$ and a frequency dependence of the flux density of $S_\nu \propto \nu^{+0.1\pm0.1}$. These indices appear to be significantly "flatter" than the values of $\theta_{maj} \propto \nu^{-0.7\pm0.1}$ and $S_\nu \propto \nu^{+0.3\pm0.1}$, found from the 1985-8 data by Rodríguez et al. (1990). Again, this suggests that small variations may have taken place in the several years that separate the two data sets. The "flat" indices found from the 1992-3 data suggest that VLA 1 was close to being an optically-thin free-free jet at that epoch.

3.2. VLA 2

This centimeter source is believed to excite the HH 144 flow (Reipurth et al. 1993, Eislöffel, Mundt, & Böhm 1994). Its flat spectral index suggests optically-thin free-free emission. Reipurth et al. (1993) find an infrared reflection nebula fanning out from VLA 2 to the west, toward HH 144. Our sensitive 3.6-cm map (Fig. 4) shows a marginal extension to the west. However, our attempts to fit the source give upper limits of $\sim 0\farcs5$ for its angular size. Moro-Martín et al. (1999) report high velocity molecular gas probably associated with the VLA 4/HH 144 system. The $H^{13}CO^+$ observations of Choi & Lee (1998) suggest that VLA 2 is more closely associated with the molecular core than VLA 1.

3.3. VLA 3

This source is associated with an H_2O maser (Ho et al. 1982) and appears to be embedded in a different core than the VLA 1 and 2 objects (Torrelles et al. 1994; Chini et al. 1997). Its flat spectral index suggests optically-thin free-free emission. VLA 3 has been

proposed to excite a powerful bipolar molecular outflow in the region (Chernin & Masson 1995, Correia, Griffin, & Saraceno 1997). Its 6-cm flux density seems to have increased significantly between the two epochs observed. A subtraction of the two 6-cm maps (see Figure 5) suggests that the flux density excess comes from the turning-on of a new, faint component to the NE of the source.

3.4. VLA 4

This radio source is a new detection, first reported here. Its centimeter position coincides within 0.″1 with the infrared position of a source first reported by Reipurth et al. (1993) and called Source 3 by them. Our 3.6-cm map (Fig. 6) suggests that it may be a double source. Again, the flat spectral index suggests optically-thin free-free emission. Reipurth et al. (1993) suggest that this source may be powering the faint object HH 146.

3.5. VLA 5

Very little is known about this source, but its negative spectral index suggests it may be a background extragalactic source.

3.6. VLA 6

Reported as a time-variable source by Rodríguez et al. (1990), curiously this source has practically identical 6-cm flux densities for 1986.2 and 1992.9. The source is unresolved, with $\theta_s \leq 0.''3$. Its negative spectral index (-0.5 ± 0.1) implies a non-thermal nature, since free-free processes cannot produce spectral indices smaller than -0.1 (Rodríguez et al. 1993).

Since the source is time-variable (at least over the epochs observed by Rodríguez et al. 1993) and it has a negative spectral index, it is possible that the source is an embedded young star with gyrosynchrotron emission from particles accelerated in situ by magnetic reconnection flares near the stellar surface. Sources of this nature have been reported and studied in several regions of star formation, including ρ Ophiuchi (André et al. 1988), Taurus (Phillips, Londsdale, & Feigelson 1993), Corona Australis (Feigelson, Carkner, & Wilking 1998), and NGC 1333 (Rodríguez, Anglada, & Curiel 1999). However, this type of non-thermal stars exhibits characteristically large circular polarizations. We searched for linear and circular polarization in all three of our data sets and did not detect any in this or any of the other sources at 3-σ levels of 33 (1986.2), 27 (1992.9), and 21 (1993.0) μJy for the Q, U, and V Stokes parameters. Alternatively, this source could be a background extragalactic source.

3.7. VLA 7

Following Rodríguez et al. (1990), we identify this source as the counterpart of HH 1F. The radio detection of only this component of HH 1 is consistent with the result of Raga et al. (1990) who show that it is the brightest knot in Hα and [OIII]. Its radio proper motion between 1986.2 and 1992.9 is shown in Fig. 7 and listed in Table 4. There is excellent agreement with the values derived from the optical over about the same period of time by Eislöffel et al. (1994). The proper motion derived for the warm molecular hydrogen associated with HH 1F (Noriega-Crespo et al. 1997) is, within the larger errors of the H_2 measurement, consistent with the optical and radio values.

3.8. VLA 8, 9, and 10

These three sources are associated with HH 2. From the results of Rodríguez et al. (1990) and Raga, Barnes, & Mateo (1990), we make the following individual associations: VLA 8 = HH 2A′, VLA 9 = HH 2H′, and VLA 10 = HH 2H. The radio detection of only these three components in the complex HH 2 object are consistent with the result of Raga et al. (1990) that they are the brightest in Hα and [OIII]. As in the optical, all three components show significant flux variations at the $\sim$30% level. In contrast with the case of HH 1, where HH 1F is the dominant condensation exhibiting very similar proper motions in radio and optical, in the case of the HH 2 radio sources we failed to find such a clear relation. Most probably, this lack of clear counterparts results from the fact that HH 2 is an extremely complicated source, breaking into many subcomponents when observed with high angular resolution and sufficient sensitivity (Schwartz et al. 1993; Hester, Stapelfeldt, & Scowen 1998). The source VLA 8, that we associate with HH 2A′, shows proper motions (see Fig. 8) of similar magnitude and nearly antiparallel to those of HH 1F (see Table 4). The proper motion reported here for HH 2A′ (μ = 0.22$\pm$0.011 arcsec year^{-1}) is significantly larger than the value of $\sim$0.07 arcsec year^{-1} reported for HH 2A by Herbig & Jones (1981). However, Eisl"offel et al. (1994) confirm the proper motion measured by Herbig & Jones for this condensation, suggesting that there is probably a combined effect of proper motion and excitation changes. This is not unexpected, since there may be areas with shock cooling times of only a few years.

The source VLA 9, that we associate with HH 2H′, has remained practically stationary. Finally, VLA 10, that we associate with HH 2H, shows proper motions consistent in absolute value with those of HH 1F and HH 2A′, but directed almost eastward. One of the subcondensations of Eislöffel et al. (1994), HH 2H2, shows similar direction of motion. Additional proper motions (Bally et al. 2000) are expected to help disentangle the

characteristics of proper motions in HH 2.

4. Conclusions

We presented new sensitive continuum observations of the HH 1-2 region at 6 and 3.6 cm. The main conclusions of our study are:

1) VLA 1, the exciting source of the HH 1-2 flow, seems to have experienced morphological changes in the period between the observations (1986.2 and 1992.9). These changes can be interpreted as produced by the motion of two bipolar knots along the jet, with proper motions comparable with those observed a few arc sec away in the optical and near-infrared knots and about one arc min away in the HH objects. We were able to identify a moving radio knot present in the 1986.2 data as a near-infrared knot (knot L of Reipurth et al. 2000) evident in 1998.2 data and displaced by about 2.″7 from the radio source. This result supports the interpretation that the knots are formed by intrinsic processes near the exciting star not by interactions with the surrounding medium.

2) The source VLA 3, associated with a water maser, also appears to have morphological changes that we attribute to the turning-on of a new component.

3) We detected a new source, VLA 4, that is the radio counterpart to source 3 of Reipurth et al. (1993) and may be powering HH 146.

4) The radio proper motions of HH 1F agree very well with values previously determined in the optical. In contrast, the radio proper motions of three components detected in associattion with HH 2 are more dificcult to understand, probably as a result of the complexity of this object.

REFERENCES

André, P., Montmerle, T., Feigelson, E.D., Stine, P. C., & Klein, K. L. 1988, ApJ, 335, 940

Anglada, G., Rodríguez, L.F., Cantó, J., Estalella, R., Torrelles, J.M. 1992, ApJ, 395, 494

Anglada, G., Villuendas, E., Estalella, R., Beltrán, M. T., Rodríguez, L. F., Torrelles, J. M., & Curiel, S. 1998, AJ, 116, 2953

Bally, J., et al. 2000, in preparation

Bohigas, J., Torrelles, J.M., Echevarría, J., Cantó, J., Enríquez, R., Firmani, C., Gutiérrez, L., Ruiz, E. Salas, L. 1985, Rev. Mexicana Astron. Astrofis. 11, 149

Böhm, K.-H., Solf, J. 1985, ApJ, 294, 533

Chernin, L.M. & Masson, C.R. 1995, ApJ, 443, 181

Chini, R., Reipurth, B., Sievers, A., Ward-Thompson, D., Haslam, C.G.T., Kreysa, E., & Lemke, R. 1997, A&A, 325, 542

Choi, M. & Zhou, S. 1997, ApJ, 477, 754

Choi, M. & Lee, Y. 1998, ApJ, 498, L71

Correia, J.C., Griffin, M., & Saraceno, P. 1997, A&A, 322, L25

Curiel, S. 1995, Rev. Mexicana Astron. Astrof. Conference Series, 1, 59

Eislöffel, J., Mundt, R., & Böhm, K.-H. 1994, AJ, 108, 1042

Feigelson. E.D., Carkner, L., & Wilking, B. A. 1998, ApJ, 494, L215

Haro, G. 1952, ApJ, 115, 572

Herbig, G.H. 1951, ApJ, 113, 697

Herbig, G.H., & Jones, B.F. 1981, AJ, 86, 1232

Hester, J.J., Stapelfeldt, K.R., & Scowen, P.A.1998, AJ, 116, 372

Ho, P.T.P., Haschick, A.D., Moran, J.M., & Rodríguez, L.F. 1982, Bull. AAS, 14, 927

Martí, J., Rodríguez, L. F., & Reipurth, B. 1998, ApJ, 502, 337

Moro-Martín, A., Cernicharo, J., Noriega-Crespo, A., Martín-Pintado, J. 1999, ApJ, 520, L111

Noriega-Crespo, A., Garnavich, P.M., Curiel, S., Raga, A.C., & Ayala, S. 1997, ApJ, 486, L55

Phillips, R.B., Lonsdale, C.J., & Feigelson, E.D. 1993, ApJ, 403, L43

Pravdo, S.H., Rodríguez, L.F., Curiel, S., Cantó, J., Torrelles, J.M., Becker, R.H., & Sellgren, K. 1985, ApJ, 293, L35

Raga, A.C., Barnes, P.J., & Mateo, M. 1990, AJ, 99, 1912

Reipurth, B., Heathcote, S., Roth, M., Noriega-Crespo, A., & Raga, A.C. 1993, ApJ, 408, L49

Reipurth, B., Yu, K.C., Rodríguez, L.F., Heathcote, S., & Bally, J. 1999, to appear in A&A

Reipurth, B., Heathcote, S., Yu, K.C., Bally, J., & Rodríguez, L.F. 2000, in preparation

Rodríguez, L.F. & Reipurth, B. 1989, Rev. Mexicana Astron. Astrofis., 17, 59

Rodríguez, L.F., Ho, P.T.P., Torrelles, J.M., Curiel, S., & Cantó, J. 1990, ApJ, 352,645

Rodríguez, L.F., Martí, J., Cantó, J., Moran, J.M., & Curiel, S. 1993, Rev. Mexicana Astron. Astrofis., 25, 23

Rodríguez, L.F. & Reipurth, B. 1996, Rev. Mexicana Astron. Astrofis., 32, 27

Rodríguez, L.F. & Reipurth, B. 1998, Rev. Mexicana Astron. Astrofis., 34, 13

Rodríguez, L.F., Anglada, G., & Curiel, S. 1999, ApJS, in press

Torrelles, J.M., Gómez, J.F., Ho, P.T.P., Rodríguez, L.F., Anglada, G., & Cantó, J. 1994, ApJ, 435, 290

Schwartz, R.D., Cohen, M., Jones, B.F., Böhm, K.-H., Raymond, J.C., Hartmann, L.W., Mundt, R., Dopita, M.A., & Schultz, A.S.B. 1993, AJ, 106, 740

Solf, J., Raga, A.C., Böhm, K.-H., Noriega-Crespo, A. 1991, AJ, 102, 1147

Strom, S.E., Strom, K.M., Grasdalen, G.L., Sellgren, K., Wolff, S., Morgan, J., Stocke, J., Mundt, R. 1985, AJ, 90, 2281

This manuscript was prepared with the AAS LaTeX macros v4.0.

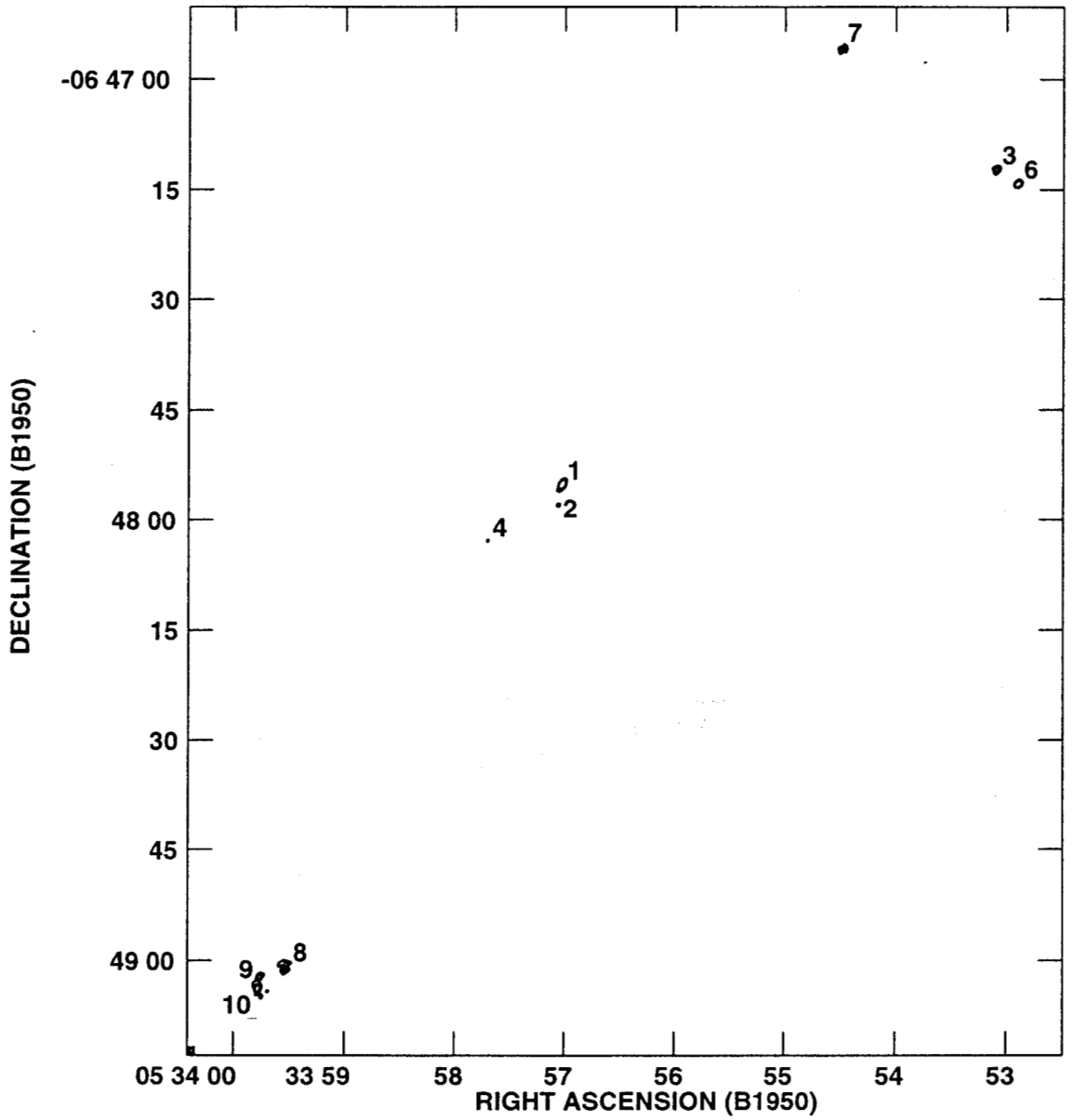

Fig. 1.— Natural-weight VLA map of the HH 1-2 region made with the 6-cm 1992.9 data. The VLA sources are indicated with their number. The source VLA 5 falls outside of the region shown, about 35″ to the west of VLA 6. The size of the restoring beam is $0\farcs63 \times 0\farcs52$, PA $= -10°$. Contour levels are -5, 5, 6, 8, 10, 12, and 15 times the rms noise of 9 μJy beam^{-1}.

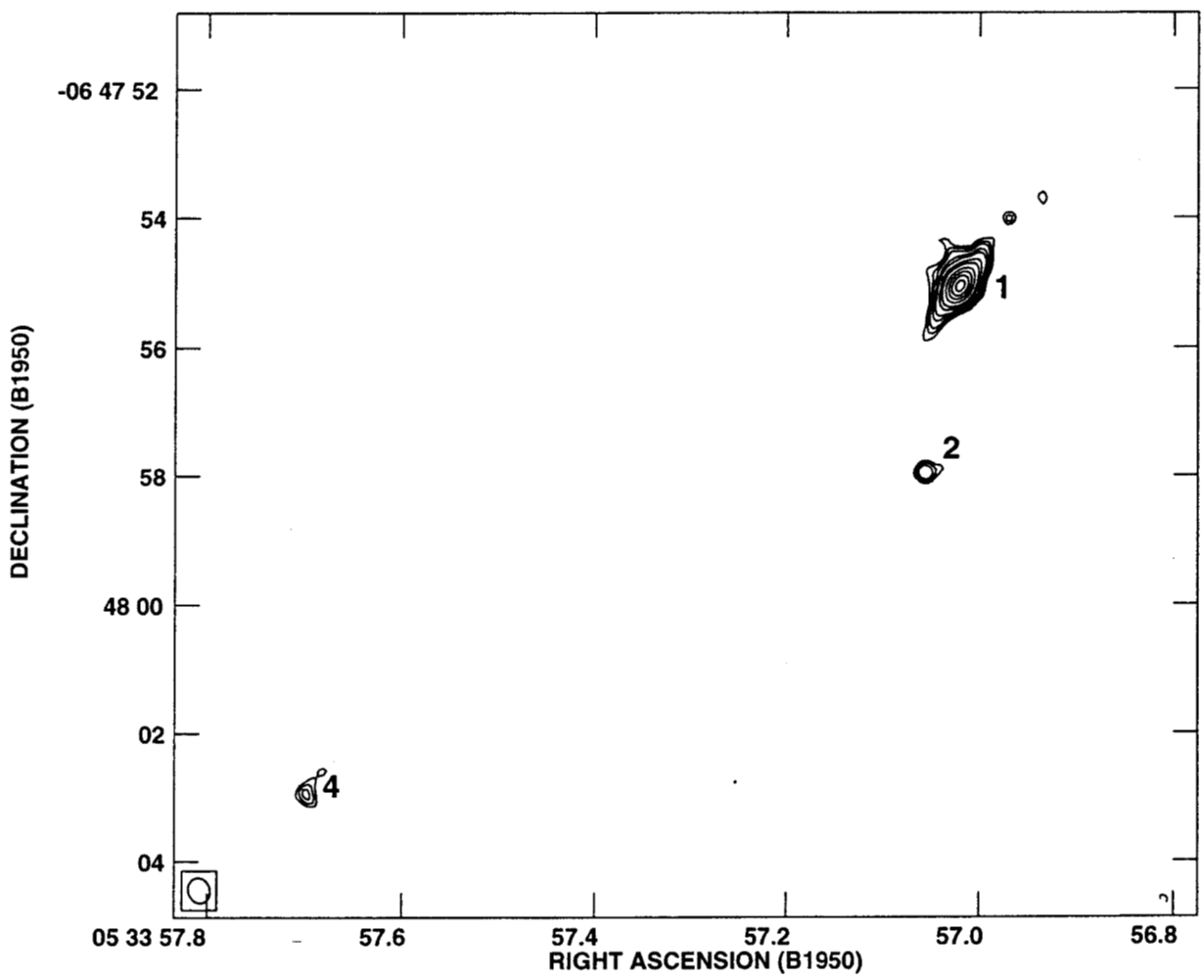

Fig. 2.— VLA map of the central part of the HH 1-2 region made with the 3.6-cm 1993.0 data and the ROBUST parameter set equal to 0. The VLA sources 1, 2, and 4 are indicated with their number. The size of the synthesized beam is $0\farcs39 \times 0\farcs33$, PA $= +19°$. Contour levels are -4, 4, 5, 6, 8, 10, 15, 20, 30, 40, 50, and 60 times the rms noise of 7 μJy beam^{-1}.

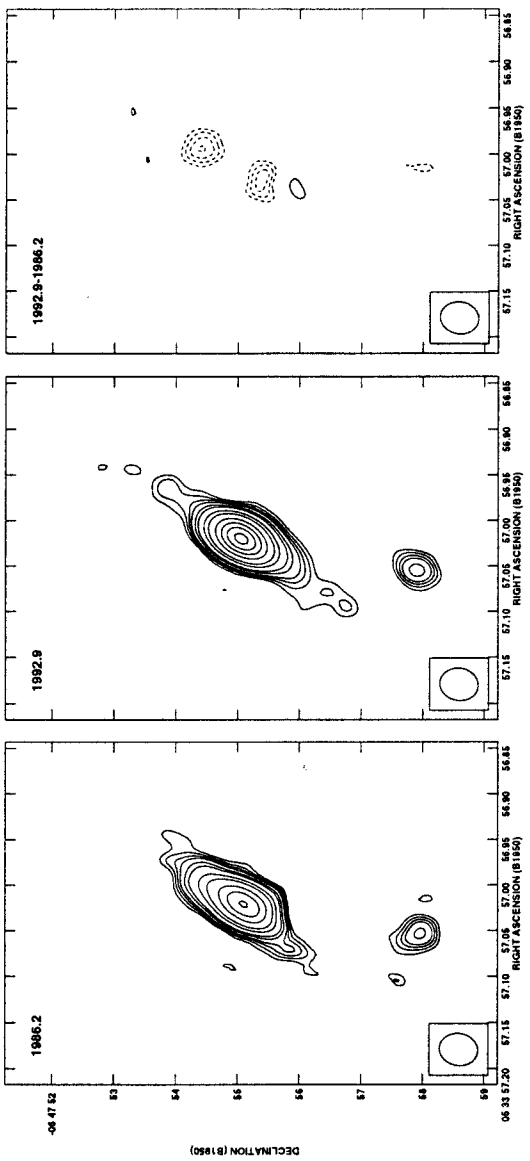

Fig. 3.— Natural weight VLA maps of the sources VLA 1 and 2, made with the 6-cm 1986.2 (left), 1992.9 (center) and 1992.9-1986.2 (right) data. The size of the restoring beam is $0\farcs63 \times 0\farcs52$, PA $= -10°$. Contour levels are 3, 4, 5, 6, 8, 10, 15, 20, 30, 40, 50, and 60 times the rms noises of 11 (1986.2 map) and 9 (1992.9 map) μJy beam^{-1}, and -6, -5, -4, -3,3, 4, 5, and 6 times the rms noise of 14 μJy beam^{-1} for the 1992.9-1986.2 difference map.

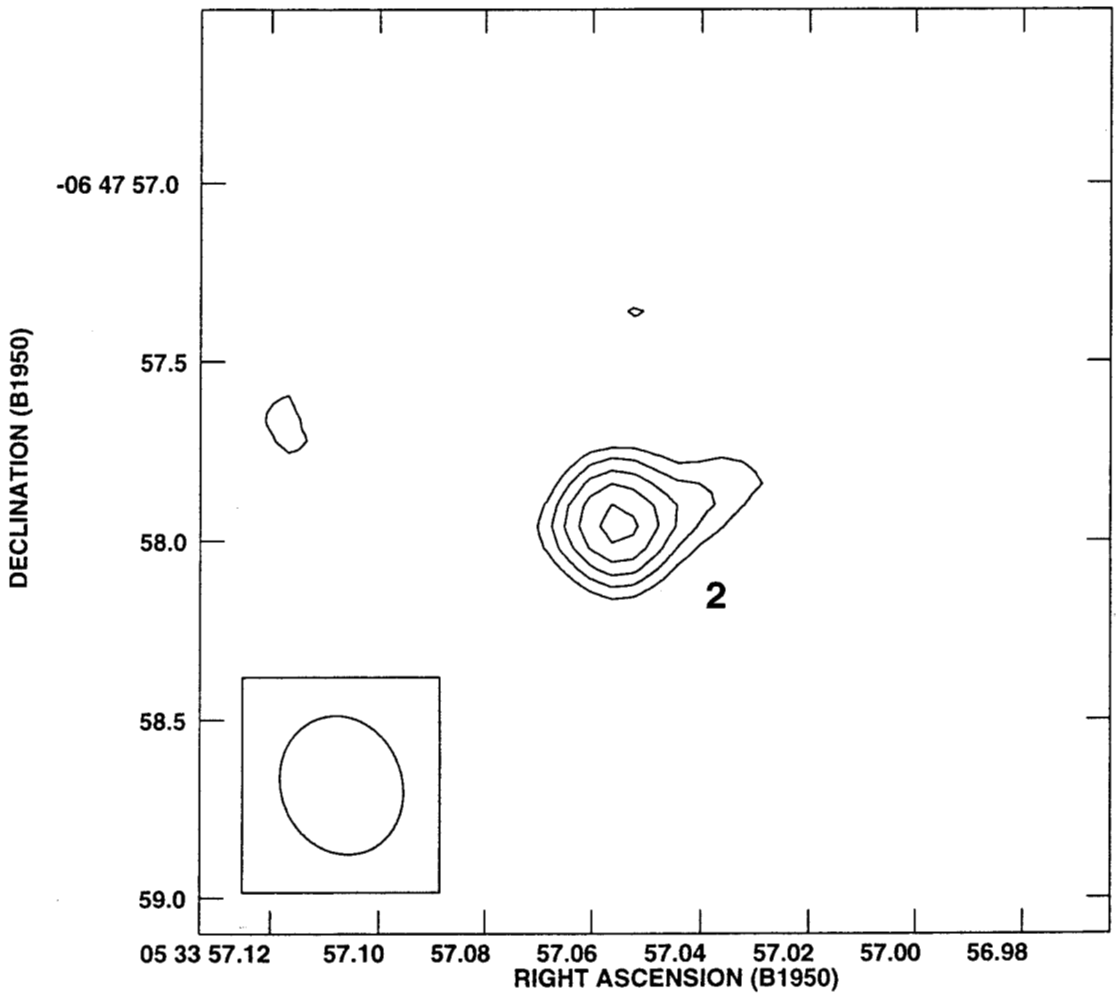

Fig. 4.— Contour map of VLA 2 made with the 3.6-cm 1993.0 data and the ROBUST parameter set equal to 0. The size of the synthesized beam is $0\farcs39 \times 0\farcs33$, PA = +19°. Contour levels are −3, 3, 4, 5, 6, and 7 times the rms noise of 7 μJy beam^{-1}.

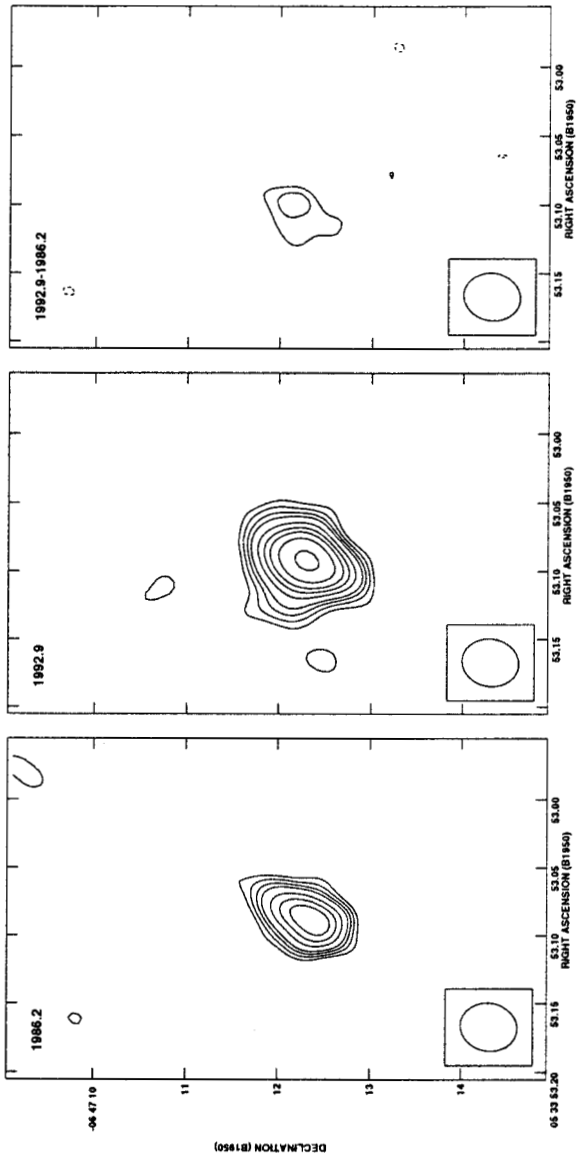

Fig. 5.— Natural weight VLA maps of the source VLA 3 made with the 6-cm 1986.2 (left), 1992.9 (center) and 1992.9-1986.2 (right) data. The size of the restoring beam is $0\farcs63 \times 0\farcs52$, PA $= -10°$. Contour levels are -3, 3, 4, 5, 6, 8, 10, 12, 15, and 20 times the rms noises of 11 (1986.2 map), 9 (1992.9 map), and 14 μJy beam^{-1} (1992.9-1986.2 difference map). The elongation of the source in the SE-NW direction is due to bandwidth smearing.

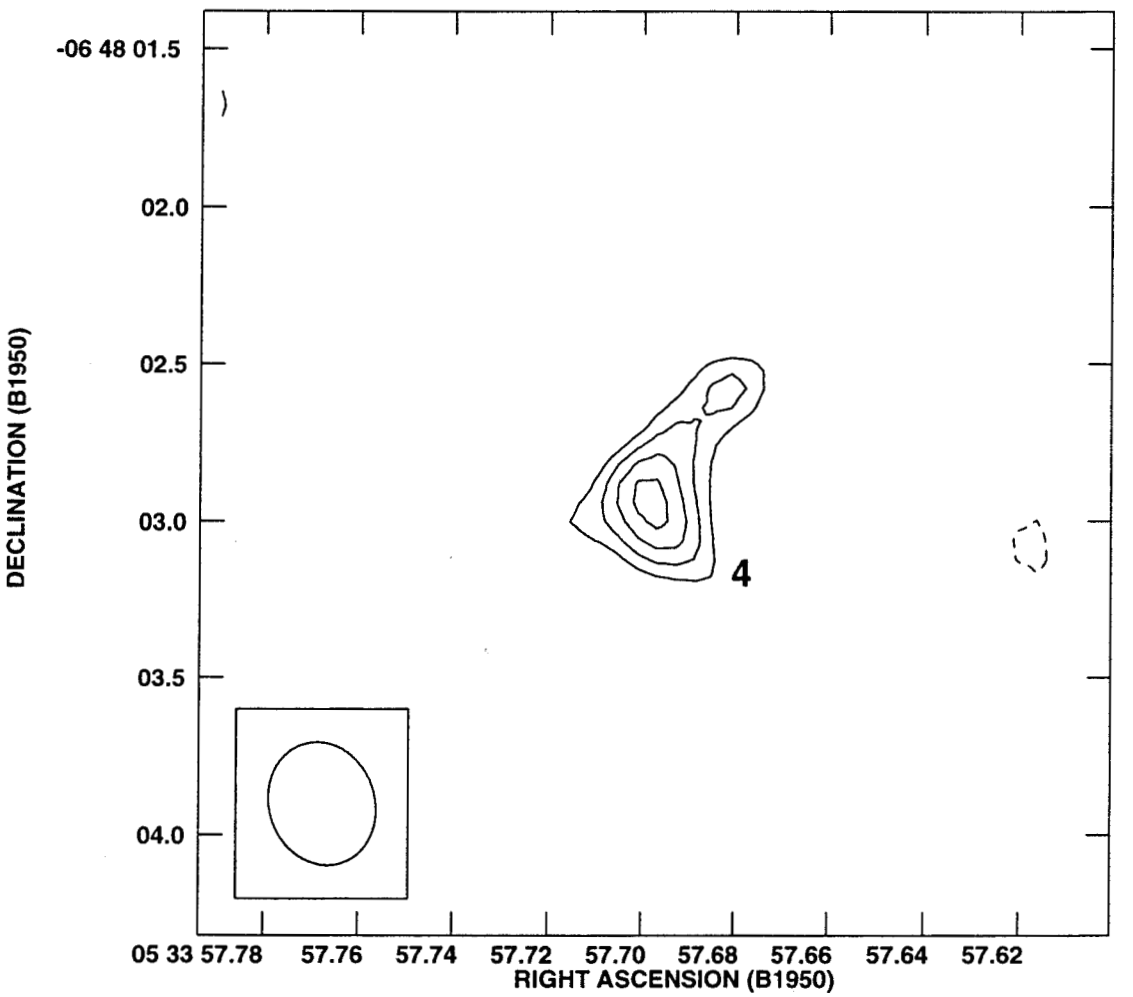

Fig. 6.— Contour map of VLA 4 made with the 3.6-cm 1993.0 data and the ROBUST parameter set equal to 0. The size of the synthesized beam is $0\farcs39 \times 0\farcs33$, PA = +19°. Contour levels are −3, 3, 4, 5, and 6 times the rms noise of 7 μJy beam^{-1}. Note that the map suggests that the source may be double.

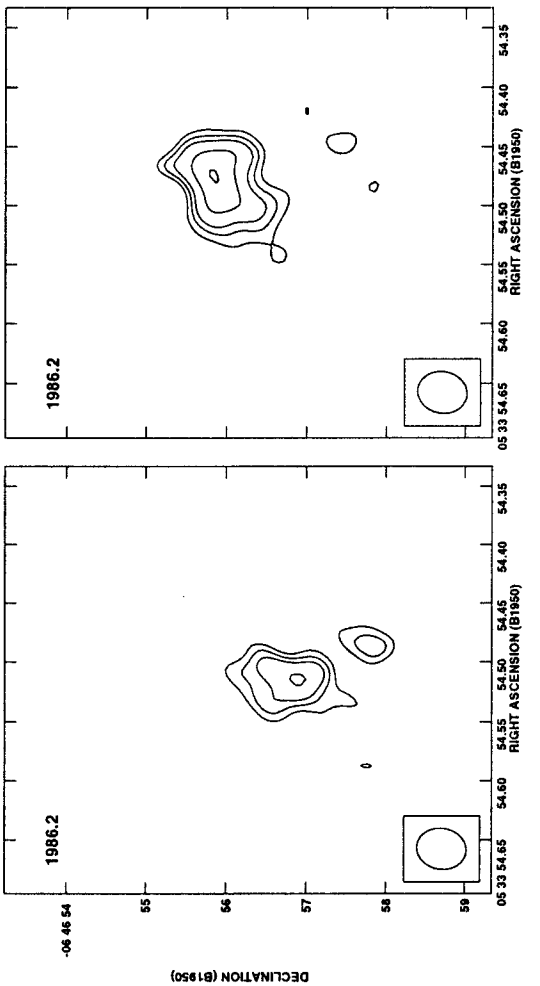

Fig. 7.— Natural weight VLA maps of the source VLA 7 (= HH 1F) made with the 6-cm 1986.2 (left) and 1992.9 (right) data. Contour levels are −4, 4, 5, 6, 8, and 10 times the rms noises of 11 (1986.2 map) and 9 (1992.9 map) μJy beam^{-1}. The proper motion of the source to the NW is evident.

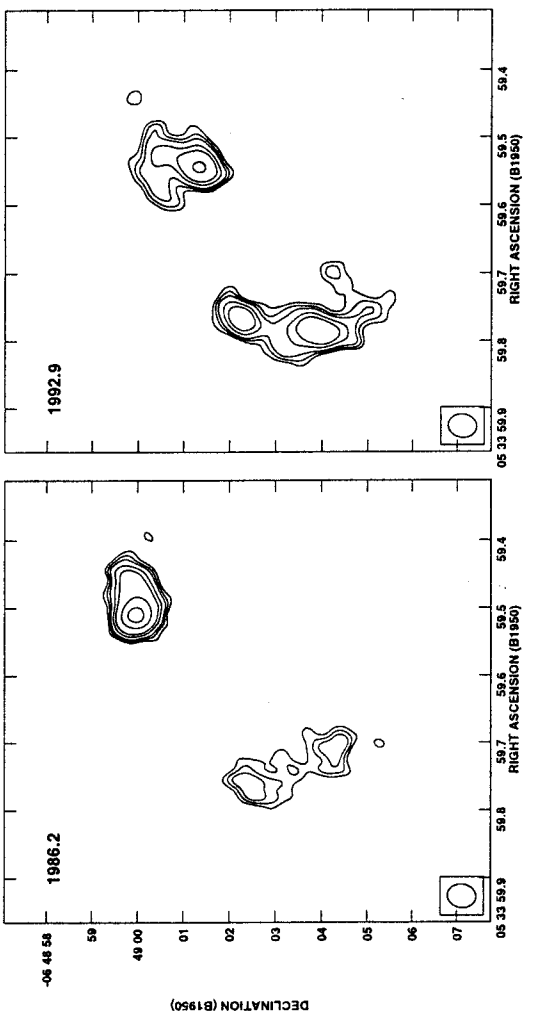

Fig. 8.— Natural weight VLA maps of the sources VLA 8 (= HH 2A′), VLA 9 (= HH 2H′), and VLA 10 (= HH 2H). made with the 6-cm 1986.2 (left) and 1992.9 (right) data. Contour levels are −4, 4, 5, 6, 8, 10, and 15 times the rms noises of 11 (1986.2 map) and 9 (1992.9 map) μJy beam^{-1}.

Table 1. SUMMARY OF OBSERVATIONS

Epoch	VLA Configuration	Wavelength (cm)	Flux Density for 0539−057 (Jy)
1986 Mar 01	A	6	1.159±0.002
1986 Mar 03	A	6	1.136±0.002
1992 Nov 02	A	6	1.005±0.002
1992 Nov 02	A	3.6	1.030±0.003
1992 Dec 18	A	6	1.126±0.001
1992 Dec 18	A	3.6	1.034±0.002
1992 Dec 19	A	6	1.144±0.001
1992 Dec 19	A	3.6	1.034±0.002
1993 Apr 30	B	3.6	0.977±0.002

Table 2. RADIO CONTINUUM SOURCES IN THE HH 1-2 REGION

	Position[a]		S_ν (mJy)[b]			Spectral	
VLA	α(1950)	δ(1950)	3.6 cm(1993.0)	6 cm(1992.9)	6 cm(1986.2)	Index[c]	Comment
5	05 33 50.501	−06 47 18.31	0.17±0.01	0.28±0.01	0.22±0.01	−0.9±0.1	Extragalactic?
6	05 33 52.890	−06 47 14.13	0.39±0.01	0.52±0.01	0.53±0.01	−0.5±0.1	Time Variable
3	05 33 53.085	−06 47 12.17	0.40±0.01	0.41±0.01	0.30±0.01	+0.0±0.1	Water Maser
7	05 33 54.482	−06 46 55.67	0.53±0.01	0.55±0.02	0.55±0.02	−0.1±0.1	HH 1F
1	05 33 57.020	−06 47 55.05	1.19±0.01	1.12±0.01	1.11±0.01	+0.1±0.1	Excites HH 1-2
2	05 33 57.054	−06 47 57.94	0.13±0.01	0.13±0.01	0.16±0.02	+0.0±0.2	Excites HH 144
4	05 33 57.698	−06 48 02.92	0.08±0.01	0.08±0.01	0.07±0.01	+0.0±0.3	IR Counterpart
8	05 33 59.551	−06 49 01.46	0.69±0.01	0.74±0.02	0.93±0.02	−0.1±0.1	HH 2A′
9	05 33 59.776	−06 49 02.45	0.29±0.01	0.30±0.01	0.41±0.02	−0.1±0.1	HH 2H′
10	05 33 59.793	−06 49 04.07	0.48±0.02	0.54±0.02	0.34±0.02	−0.2±0.1	HH 2H

[a] Positions are from the 1993.0 map at 3.6-cm. The positional error is estimated to be typically $\sim 0''.05$.

[b] Total flux densities corrected for the primary beam response.

[c] Spectral indices from the 1992.9 map at 6-cm and the 1993.0 map at 3.6-cm.

Table 3. ANGULAR DIMENSIONS AND POSITION ANGLE OF VLA 1[a]

Epoch	Wavelength (cm)	Major Axis (arc sec)	Minor Axis[b] (arc sec)	Position Angle (degrees)
1986.2	6	0.87±0.04	≤0.23	143±1
1992.9	6	0.61±0.04	≤0.25	142±2
1993.0	3.6	0.55±0.03	≤0.09	141±1

[a]From Gaussian ellipsoid fits to the u,v data.

[b]Upper limits at the 3-σ level.

Table 4. PROPER MOTIONS OF HERBIG-HARO OBJECTS[a]

Object	μ (arcsec year^{-1})	PA(°)
HH 1F	0.18±0.01	331±4
HH 2A′	0.22±0.01	160±4
HH 2H′	0.03±0.01	54±30
HH 2H	0.19±0.01	70±4

[a]From 6-cm 1986.2 and 1992.9 data.